TELKOMNIKA Telecommunication, Computing, Electronics and Control
Vol. 18, No. 4, August 2020, pp. 1968~1975
ISSN: 1693-6930, accredited First Grade by Kemenristekdikti, Decree No: 21/E/KPT/2018
DOI: 10.12928/TELKOMNIKA.v18i4.14828

Incident and reflected two waves correlation with cancellous bone structure

Muhamad Amin Abd Wahab, Rubita Sudirman, Mohd Azhar Abdul Razak, Fauzan Khairi Che Harun, Nurul Ashikin Abdul Kadir, Nasrul Humaimi Mahmood
School of Electrical Engineering, Faculty of Engineering, Universiti Teknologi Malaysia, Malaysia

Article Info

Article history:

Received Aug 27, 2019
Revised Feb 25, 2020
Accepted Apr 7, 2020

Keywords:

Bandlimited deconvolution
Fast and slow wave
Pulse echo
Through transmission
Ultrasound

ABSTRACT

The correlation in bone microstructure for ultrasound pulse echo technique is still less accurate compared to through transmission technique. Previous works demonstrated, reflected two modes wave has significant association with bone porosity. The paper aims is to conduct simulation using pulse echo technique to examine the relationship between fast and slow waves with porosity of 2-dimensional cancellous bone models by comparing the result to through transmission technique. The "incident" and "reflected" waves were separated using bandlimited deconvolution method by estimating time threshold of fast and slow waves' transfer function. The parameters of the waves were computed, plotted versus porosity for six different thicknesses and the correlation coefficients between them were compared. The incident and reflected fast wave attenuations show marginally significant correlation with porosity for both bone models orientations. Wave propagation for parallel orientation dominated by incident and reflected fast wave, meanwhile, perpendicular orientation dominated by incident slow wave. The thickness factor affected wave amplitude but less affected the attenuation. Because of propagation loss, reflected wave shows lower correlation to porosity compared to incident wave. Hence, analyzing fast and slow waves might improve the measurement accuracy of pulse echo technique compared to using single mode wave to estimate bone quality.

Corresponding Author:

Rubita Sudirman,
Department School of Electrical Engineering, Faculty of Engineering,
Universiti Teknologi Malaysia,
81310 UTM Johor Bahru, Malaysia.
Email: rubita@fke.utm.my

1. INTRODUCTION

Many applications in engineering, medicine [1], biology, and so on [2] using ultrasound technology in their system for certain purposes. Previous study indicate that, the parameters of fast and slow waves was associate more with the internal structure (microstructure) of the cancellous bone [3-9] and analysis these waves could improve bone quality estimation via ultrasound. The anisotropy of cancellous bone can affect time domain observation of fast and slow wave and most of the time, these waves overlapped with each other [10]. Numerous techniques to decompose fast and slow wave were created by Wear and among them was bandlimited deconvolution method. This method was simple to implement compare to other complex methods such as Bayesian method [8, 11, 12]. This method also effectively decomposes fast and slow waves, yet only implemented in through transmissions (TT) evaluation technique.

Nonetheless, the TT technique was the only technique which widely used to investigate fast and slow wave. However, it is difficult to perform bone health assessment at specific skeletal part such as hip and backbone, due to the TT technique required a pair (two) of transducers to function [3, 13]. Because of that, the pulse echo (PE) evaluation technique is suggested to resolve these complications, since the technique simply uses single transducer, where it much easier to evaluate bone assessment at the hip and backbone. However, the accuracy of PE technique is still not powerful compared to TT technique because of the complex behavior of reflected and backscattered wave relation with inhomogeneity of cancellous bone. Therefore, using the finite difference time domain simulation (FDTD), Hosokawa demonstrate that, fast and slow wave can be isolated from reflected/backscattered wave and related more with bone porosity and this finding might improve the PE technique for bone quality estimation [3, 13-15].

Thus, the objective of this paper is to perform a 2-dimentional (2-D) simulation using PE technique to examine the relationship of fast and slow wave with structure orientation, porosity, and thicknesses of cancellous bone models and the result is compared with TT technique. The correlation coefficient (R^2) will be used to determined the the accuracy of correlation between wave's parameters and porosity. Fast and slow wave will be predicted for both measurement techniques via bandlimited deconvolution method. Previously, no research has used bandlimited deconvolution method to decompose reflected mix waves into two individual reflected fast and slow waves. Afterwards, the parameters of single modes (mix), fast and slow waves for both techniques will be compared in term of their correlation coefficient in order to determine which waves was correlate more with microstructure of bone models.

2. RESEARCH METHOD

2.1. Simulation setup and wave measurement technique

The software SimNDT version 0.43 was used for this analysis [16]. The single Gaussian sine wave with 1 MHz of frequency was set as output pulse for the transducer and simulation setup was based on TT and PE technique. Refer to the Figure 1, the size of planar-type transducer was (length) 5.5 mm. The second transducer for the TT technique was located below the cancellous bone models. For the PE technique, below the cancellous bone models was air-water boundary that acts as reflector element. The simulation time for TT and PE was set to 25 and 40 µs, respectively. The 20 Volt peak-to-peaks (V_{pp}) was set for the input voltage source. The distance between the bone models and transducer was 8 mm and the absorbing layer with the thickness of 5 mm was covered the simulation area. Table 1 shows the acoustic and material properties of bone and water based on paper from Nagatani et al. [17].

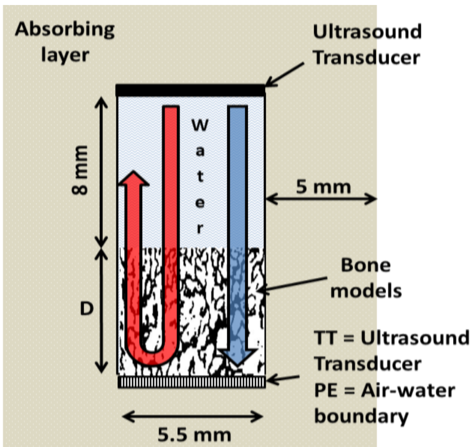

Figure 1. Simulation setup diagram
(the blue arrow corresponds to incident wave and red arrow corresponds to reflected wave)

Table 1. Acoustic and material properties

Material	Density (g/cm^3)	Velocity (m/s)
Bone	2000	Longitudinal: 3500 Shear: 2400
Water	1000	Longitudinal: 1497 Shear: 0

2.2. 2-D bone models

The 2-D cancellous bone models used in this simulation was originated from paper Gilbert et al. [18]. There are 9 models for each parallel and perpendicular orientation. For each model, there are 6 different thicknesses, ranging from 5 to 10 mm. The geometric scenario's size of the 2-D bone model's image was set to 170×125 pixel, whereas, 25 pixel/mm was set for the whole simulation area. The porosity level of bone models was ranging from 30% to 75% and was measured by using ImageJ software based on image color threshold. Refer to Figure 2, the parallel model was refer to the trabecular shape that was parallel with the direction of wave propagation (arrow) and vice versa for perpendicular models.

2.3. Bandlimited deconvolution method and wave parameters

There are no attempts yet to implement this method toward the reflected wave. Hence, this paper can show the feasibility of this method to decompose reflected fast and slow wave. The frequency-dependent of wave reaction for the bone can be defined by,

$$Y(f) = X(f)[Hfast(f) + Hslow(f)] \tag{1}$$

where the $Y(f)$ is the spectrum of the wave propagate through a bone models (mix wave) and $X(f)$ is the spectrum of the wave propagate through water only (reference wave). The f is the ultrasound frequency. The transfer function, $Hfast(f)$ and $Hslow(f)$ for porous structure were considered as two waves propagating at the same time through an attenuating medium [19] and the detail of the method can be referred in [11, 12]. In summary (Figure 3), the time domain mix (incident/reflected), $x(t)$ and reference wave (incident/reflected), $y(t)$ was converted to frequency domain signal, $X(f)$ and $Y(f)$ via fast Fourier transform (FFT). Then, $Htotal(f)$ was calculated by divided $X(f)$ by $Y(f)$. The bone impulse response, $htotal(t)$ was converted from $Htotal(f)$ by using inverse FFT (IFFT). Then, based on a time threshold of local minimum (wave envelope) determined by the time shifts parallel to velocities above 1479 m/s (reference wave), a rectangular time-domain windows will be created. The time threshold above velocities of reference wave was chosen because the velocity of fast wave was expected to be faster compared to wave through water only. To estimate the fast wave impulse response, $hfast(t)$, the $htotal(t)$ was multiplying with time domain window with a value equal to one for times before the threshold and zero for times after the threshold. To obtained slow wave impulse response, $hslow(t)$, $hfast(t)$ was subtracted by $htotal(t)$ due to relation in (1). After that, the slow wave transfer function, $Hslow(f)$ was converted from $hslow(t)$ via FFT and multiply with $X(f)$ in order to obtained frequency domain's predicted slow wave, $Yslow(f)$. To get $yslow(t)$ (slow waves in time domain), the IFFT computation will used against the $Yslow(f)$ and to obtain fast wave in time domain, $yfast(t)$, simply subtract $yslow(t)$ with $y(t)$.

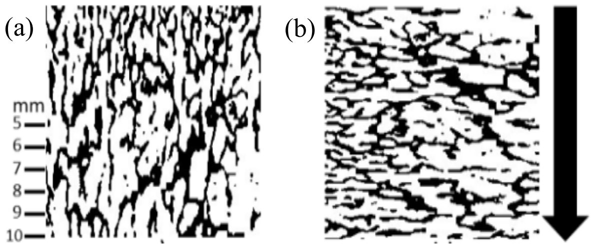

Figure 2. Examples of (a) parallel model and (b) perpendicular model (black = solid trabecular). Arrow is the direction of wave

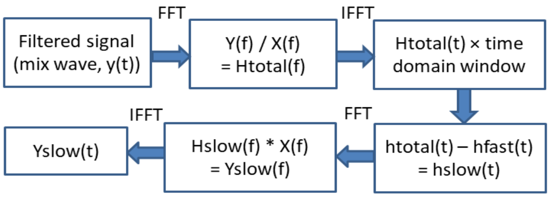

Figure 3. The process flow of the bandlimited deconvolution method [11, 12]

Wave amplitude (A) (frequency domain peak value of signal amplitude) and frequency dependent attenuation (β) were considered in the simulation work, where β is given by,

$$\beta(f) = \frac{1}{D}\left[20\log SR(f) - 20\log SB(f)\right] \tag{2}$$

where $SR(f)$ and $SB(f)$ is the spectrum of wave propagate through water and bone models, respectively. The D is the thickness of bone models in cm. The frequency range for the slope $\beta(f)$ was from 0.2 MHz to 0.6 MHz and the unit was dB/cm/MHz.

3. RESULTS AND ANALYSIS

3.1. Separation of fast and slow wave

The typical incident wave obtained from TT measurement technique was shown in Figure 4. For the parallel bone models, at the time of 14 µs, there are two modes of waves, specifically fast and slow wave. However, only single mode wave was observed for the perpendicular bone model. The slow wave also has bigger amplitude than the fast wave. This is due to the propagation of the fast wave through solid trabecular of cancellous bone, and experienced a higher attenuation affect compared to slow wave, where these waves (slow wave) propagate through of pore part of cancellous bone (lesser attenuation effect media) [10]. The separation of fast and slow wave in the time domain as shown in Figure 4 for parallel orientations was in good agreement with previous investigations by Hosokawa [10, 20]. For the incident wave with parallel orientation, the incident fast and slow wave were estimated based on observation in time domain, not using bandlimited deconvolution.

Figure 5 (a) shows an example of the bone impulse response, $htotal(t)$ or $h(t)$ of the TT measurement technique for the perpendicular orientation of bone models. The $|h(t)|$ was the envelope of $htotal(t)$. The time threshold that split the bone impulse response into $hfast(t)$ (left) and $hslow(t)$ (right) was specified by the vertical dashed line (red). The arrival time of incident fast wave was approximately 0.38 µs (*tFast*) earlier, whereas the arrival time of incident slow wave (estimated by *yslow(t)*) was 0.66 µs (*tSlow*) late compare to incident reference wave adjustment measurement arrival time (i.e., time, *tRef* = 0 µs).

Figure 5 (b) shows $yslow(t)$, incident mix (red + blue), first and second waves estimated using bandlimited deconvolution method. The $yslow(t)$ was used to estimate the possibility of time-domain location of slow wave from mix wave. Then, the fast wave was obtained by subtracted the slow wave from the mix wave. Referring to Figure 6 (a) and Table 2 for the porosity value of 67%, the amplitude of incident mix wave was 0.82 V. The amplitude of incident slow wave was higher (0.64 V) than the incident fast wave (0.22 V). Previous work by Nagasaki et al. [4], Kawasaki et al. [5], Otani [6], Cardoso et al. [7] and Nelson et al. [8] also report the same findings in terms of amplitude ratio of fast and slow waves.

Moreover, the oscillation frequency of $hslow(t)$ (based on $|h(t)|$) was higher than that for $hfast(t)$ as shown in Figure 5 (a) and the slope of attenuation for the incident slow wave (91 dB/cm/MHz) was lower than that for the incident fast wave (118 dB/cm/MHz) which also shown in Figure 6 (b) and Table 2. The same behaviors of fast and slow waves were also reported from the previous research [11]. The relation of the lower frequency and higher attenuation of the fast wave is due to high frequency component of wave affected more by attenuation, specifically absorption compared to the low frequency component [21]. Nonetheless, some situation exhibits amplitude of fast wave bigger or similar with slow wave depends on density and the acoustic properties of bone phantom or material used [22, 23].

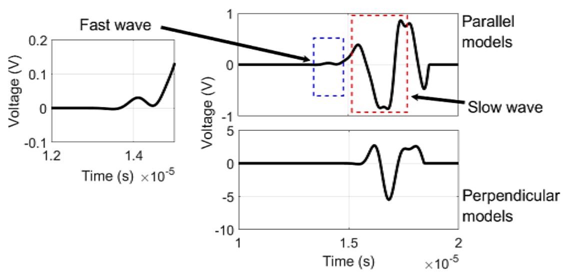

Figure 4. Example of incident wave propagates through parallel and perpendicular orientation

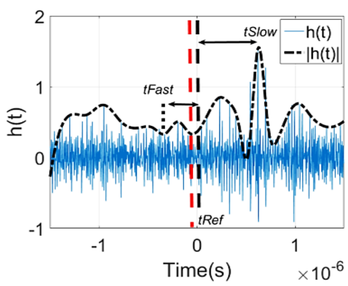

(a)

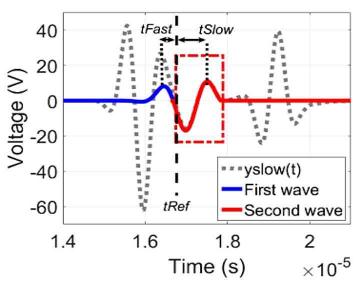

(b)

Figure 5. Examples of (a) transfer function and (b) incident first and second wave for the perpendicular orientation bone models (porosity = 67%, thickness = 5 mm)

Table 2. Data related to Figure 6

P (%)	A (V)			β (dB/cm/MHz)		
	Mix	Fast	Slow	Mix	Fast	Slow
33	0.32	0.25	0.09	56	95	124
36	0.48	0.26	0.23	70	95	115
37	0.41	0.43	0.03	69	57	124
49	0.38	0.22	0.17	63	80	79
53	0.77	0.17	0.62	57	101	88
54	0.80	0.16	0.64	52	113	87
67	0.82	0.22	0.64	42	118	91
71	1.30	0.29	1.08	49	118	85
74	1.77	0.33	1.47	51	116	82

P = Porosity, A = Amplitude and β = Attenuation

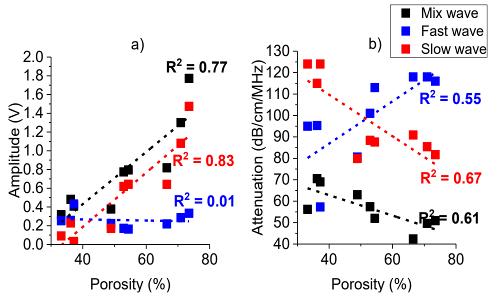

Figure 6. Example of (a) amplitude and (b) attenuation versus porosity of incident wave

3.2. Correlation of the wave parameters with various porosities and thicknesses

Referring to Table 3 – TT – parallel orientation sections, the amplitude of the incident slow wave and mix (*AIslow* and *AImix*) increased when porosity increases for all thickness. The correlation coefficient for both waves also seems to decrease when thickness decrease. However, there is no or low correlation between attenuation of the incident mix and slow waves (*βImix* and *βIslow*) and porosity. The amplitude of incident fast waves, *AIfast* decrease when porosity increase and the correlation coefficient increase when thickness decreases. The attenuation of the incident fast wave, *βIfast* increases with porosity with consistent and slightly significant correlation coefficient for all thicknesses.

In the Table 3 – TT – perpendicular orientation, the *AImix* and *AIslow* increase when porosity increases while *βImix* and *βIslow* decrease when porosity increase. Both incident mix and slow waves parameters show high correlation coefficient and consistent for all thicknesses. Nevertheless, the *AIfast* also increase when porosity increases for all thicknesses except at the thickness of 5 mm. The correlation coefficient also decreases when thickness increase. In terms of *βIfast*, this parameter shows an increasing trend versus porosity with slightly significant and consistent correlation coefficient for all thicknesses. Figures 6 (a) and (b) show examples of the correlation between the two parameters (amplitude and attenuation of incident wave) and porosity for parallel orientation of bone models with porosity value of 67% and thickness of 5 mm.

As shown in Table 3 – PE – parallel orientations, the amplitude of the reflected mix wave, *ARmix* decrease when porosity increases. However, the correlation coefficient is slightly low for all thicknesses. The attenuation of the reflected mix wave, *βRmix* increase when porosity increases. The correlation coefficient was slightly significant at the thickness of 5 mm, but low to the rest of thicknesses. In addition, the amplitude of the reflected fast wave, *ARfast* decreases when porosity increases and the correlation coefficient was slightly significant. The *ARfast* also seems not affected by changes of thickness. In terms of attenuation of the reflected fast wave, *βRfast* increase when porosity increase with low correlation at the thicker bone models, but the correlation coefficient increase when thickness decreases. On the other hand, both parameters of the reflected slow wave (*ARslow* and *βRslow*) show no correlation with porosity. Refer to Table 3 – PE – perpendicular orientations, all wave amplitudes show low correlation versus porosity. The *βRmix and βRslow* also show low correlation versus porosity. However, the *βRfast* shows negative trends versus porosity with slightly significant correlation coefficient versus porosity for all thicknesses.

The decreasing trend of *AIfast* and *ARfast* for parallel orientation versus porosity corresponds to the behavior of fast wave was reported by Hosokawa et al. [10], Kawasaki et al. [5] and Otani [6]. As mention previously, the fast wave propagates mainly through solid trabecular. When porosity increase, the solid trabecular decrease, thereby, reduces the medium for fast wave to propagate which contribute to low amplitude. The opposite happens to the increasing trend of *AIslow* for parallel orientation versus porosity which due to the slow wave propagates through pore part of porous structure. When trabecular spacing and pore size growth, it boosts the flow of the fluid, which reduces the opposition of wave propagation, resulting in decreasing of the attenuation effect [24]. Previous research by Hosokawa et al. [10], Kawasaki et al. [5] and Otani [6] also reported the same outcome for the slow wave.

For the parallel orientation, the increasing trend of *βIfast* and *BRfast* was corresponded with the decreasing trend of *AIfast* and *ARfast.* When the amplitude decreases, the attenuation was expected to increase. Nevertheless, Hoffman et al. [25] described that, due to bone sonometry effect, the fast wave slope of attenuation decrease when porosity increases. Moreover, Cardoso et al. [7] specifies that, the the fast wave slope of attenuation was displaying parabolic manners versus porosity, which due to domination of slow wave slope of attenuation against most of the frequency ranges, mainly for the cancellous bone with higher porosity level. In this paper, the parallel orientation has continuity of connection between solid trabecular might enhance the propagation of reflected and incident fast wave and these waves usually has lower frequency content.

Because of that, the frequency of ranges (0.2 – 0.6 MHz) for the slope of attenuation might be dominated by fast wave and causing *βIslow* and *βRslow* to show low correlation with porosity. Furthermore, for perpendicular orientation, the *βIslow* shows a behavior similar with slow wave as found from previous research by Hoffman et al. [25] and corresponded with the increasing *AIslow* versus porosity. The high correlation coefficient of *βIslow* also supports the claim that slow wave may be dominating the incident wave propagation for perpendicular orientation. Same goes to *ARfast* for parallel orientation, which dominate the reflected wave propagation. Because of that, the *ARfast* and *ARmix* show similar trend versus porosity compared to *ARslow*.

Table 3. Overall result of correlation coefficient for TT and PE measurement technique

P	D	BO	Correlation Coefficient, R^2						BO	Correlation Coefficient, R^2					
			TT (*I*)			PE (*R*)				TT (*I*)			PE (*R*)		
			M	*F*	*S*	*M*	*F*	*S*		*M*	*F*	*S*	*M*	*F*	*S*
A	10	∥	0.50	-0.28	0.51	-0.47	-0.57	0.02	⊥	0.80	0.51	0.81	-0.01	-0.02	0.01
	9		0.33	-0.21	0.51	-0.27	-0.42	0.05		0.79	0.57	0.77	-0.04	0.19	-0.03
	8		0.32	-0.51	0.45	-0.28	-0.37	0.01		0.80	0.39	0.81	-0.05	-0.01	-0.02
	7		0.18	-0.74	0.32	-0.28	-0.29	0.02		0.77	0.31	0.79	-0.04	-0.02	-0.03
	6		0.12	-0.77	0.36	-0.35	-0.36	-0.07		0.67	0.01	0.70	-0.10	-0.16	-0.02
	5		0.01	-0.64	0.32	-0.33	-0.37	-0.02		0.78	-0.01	0.83	-0.22	-0.51	-0.01
β	10	∥	-0.08	0.57	0.02	0.33	0.37	-0.06	⊥	-0.92	0.41	-0.76	-0.01	0.45	0.02
	9		-0.01	0.58	-0.20	0.09	0.44	-0.13		-0.45	0.48	-0.50	0.05	0.47	0.20
	8		-0.01	0.40	-0.20	0.07	0.43	-0.01		-0.64	0.49	-0.76	0.11	0.40	0.17
	7		-0.01	0.68	-0.26	0.13	0.71	0.01		-0.63	0.41	-0.79	0.15	0.60	0.10
	6		-0.18	0.45	0.02	0.28	0.71	0.01		-0.69	0.65	-0.55	0.10	0.46	-0.01
	5		-0.01	0.51	-0.06	0.58	0.57	0.08		-0.61	0.55	-0.67	0.36	0.32	-0.02

- BO = Bone orientation, ∥ = parallel, ⊥ = perpendicular, P = Parameters, D = Thickness (mm), A = Amplitude, β = Attenuation, M = Mix wave, F = Fast wave, and S = Slow wave.
- Sign (±) specify positive or negative trend versus porosity
- n = 9; Very significant: $R^2 \geq 0.798$, $p \leq 0.01$; Significant: $R^2 \geq 0.666$, $p \leq 0.05$; Slightly significant: $R^2 \geq 0.348$, $p \leq 0.1$

The trend of *βIfast* is not parallel with the trends of *AIfast* for perpendicular orientation. However, the trend of *βIfast* for perpendicular orientation was the same as *βIfast* for parallel orientation. This indicates that, the slope of attenuation not influenced by amplitude. Not only that, the *βRfast* for parallel and perpendicular orientations also behaves the same as *βIfast*. This behavior might be due to scattering effect from acoustic impedance mismatch and inhomogeneity of trabecular structure [26, 27] especially at high porosity was affected fast wave, thereby, showing an increasing trend versus porosity for attenuation of fast wave, despite some situation, where the behavior of the amplitude of fast wave not correspond with the attenuation. Meanwhile, absorption, which was caused by natural absorption in the solid and liquid phase (bone marrow or water) [26] may affect slow wave. The total attenuation mostly contributes by scattering effect compared to absorption at the higher porosity bone models.

In terms of performance of the correlation coefficient, overall result shows that the incident wave has good correlation with porosity compared to reflected wave. This might be due to propagation loss of reflected wave suffered. The reflected waves propagate through bone, reflected at the boundary between air and water was weakened the reflected wave. After that, these waves propagate again through bone before reaching transducer. Not only that, the reflected wave also may be mixed with scattered wave inside a cancellous bone structure (produced by the propagation of incident wave) and deteriorate the reflected wave.

Previous research by Nagatani et al. [17] shows that the attenuation of fast wave increases when thickness increases and then the attenuation decrease to certain value and become constant. It specifies that fast wave required certain thickness to generate when ultrasound waves propagate through cancellous bone [17]. Nelson et al. [28] indicate that, attenuation in frequency domain (slope of attenuation) of fast and slow wave was constant for cancellous bone thickness from 5 mm to 15 mm. Moreover, in time domain analysis (ratio of amplitude between sample and reference wave), the attenuation of fast wave decrease considerably when thickness increase while attenuation of slow wave decrease slightly. This behavior occurs for the attenuation in time domain because of the nature of broadband pulse [28]. This behavior also might be the reason why correlation coefficient of *AIfast* for parallel orientation decreases when thickness increases. At the lesser thickness, the fast wave shows a clear difference of amplitude for each porosity value. But, when thickness increases, the difference of amplitude for each value is reduce, hence, causing less clear of trends as well correlation coefficient to decrease. Same goes to the correlation coefficient of *AIfast* for perpendicular orientation which seems to show trend changes from increase to decrease when thickness decrease.

Besides, the *βIfast* and *βRfast* for parallel and perpendicular orientation also shows consistent in correlation coefficient when the thickness increases. This shows that, the attenuation in frequency domain (slope of attenuation) not really affected by the thickness. Next, the decreasing of the correlation coefficient of *AIslow* for parallel orientation when thickness increase may be due to increases of solid trabecular which affected amplitude of slow wave. But, the correlation coefficient of *βIslow* for parallel and perpendicular was assumed consistent despite for low correlation for parallel orientation. However, the correlation coefficient of *AIslow* for perpendicular orientation appears consistent when thickness increases. This behavior may be due to slow wave domination and the effect of attenuation in the time domain which not affects much slow wave as found by Nelson et al [28]. For the parallel orientation, the correlation coefficient of *ARfast* decreases slightly when thickness increases, where the behavior was a bit different compared to *AIfast*. The domination of *ARfast* as mention previously may contribute such behavior of this wave for all thicknesses.

However, the interaction between reflection wave and cancellous bone needs to be further investigated to better understand its behavior. The propagation loss and multiple scattering may be involved and need to be solved before broadband deconvolution method was applied to reflected wave and perhaps can produce a clear correlation between reflected fast and slow wave and porosity. The 2D simulation environment may not be as powerful as 3D simulation and real experiment, hence, the result might be a bit different with other research.

4. CONCLUSION

In conclusion, the reflected fast and slow wave was possible to be separated using bandlimited deconvolution, where there was no attempt before by other researchers to decompose the reflected wave using this method. Besides, this paper also shows a behavior of the reflected fast and slow waves, which might be useful to other researchers to further investigate as the purpose to improved accuracy of bone estimation using pulse echo technique. Moreover, the attenuation of incident and reflected fast wave for both bone orientations showing a similar increases trend versus porosity with a slightly good correlation coefficient. This was due to solid structure of bone was related to fast wave. The incident slow waves dominated the wave propagation for perpendicular orientation for both parameters and showing good correlation with porosity. The behavior of slow wave indicates that, pore part of the bone was related with this wave. In addition, the thickness of bone models clearly affected incident fast and slow wave in terms of amplitude but less effect in terms of attenuation which is good agreement with previous research, where attenuation behave constantly when thickness increase. The orientation of bone models also affected both reflected and incident fast and slow waves. The complex behavior of reflected wave interacts with inhomogeneity of cancelous bone models still difficult to interpret due to propagation loss suffered by these waves. However, the accuracy of bone health evaluation for pulse echo technique might improve if considering two modes wave instead of single mode especially fast wave.

ACKNOWLEDGEMENT

The researchers would like to thank Universiti Teknologi Malaysia (UTM) and MOHE for funding the study under grant Vot Q.J13000.2551.21H49 and Q.J13000.3001.01M13.

REFERENCES

[1] Chijindu V., Udeze C., Ahaneku M., Anoliefo E., "Detection of Prostate Cancer Using Radial/Axial Scanning of 2D Trans-rectal Ultrasound Images," *Bulletin of Electrical Engineering and Informatics*, vol. 7, no. 2, pp. 222-229, 2018.

[2] Toufik Merdjana A. C., "Study and simulation with VHDL-AMS of the electrical impedance of a piezoelectric ultrasonic transducer," *International Journal of Power Electronics and Drive System (IJPEDS)*, vol. 10, no. 2, pp. 1064-1071, 2019.

[3] Hosokawa A., "Numerical Analysis of Ultrasound Backscattered Waves in Cancellous Bone Using a Finite-Difference Time-Domain Method: Isolation of the Backscattered Waves From Various Ranges of Bone Depths," *IEEE Transactions on Ultrasonics, Ferroelectrics, and Frequency Control*, vol. 62, no. 6, pp. 1201-1210, 2015.

[4] Nagatani Y., Nguyen V. H., Naili S., Haïat G., "The effect of viscoelastic absorption on the fast and slow wave modes in cancellous bone," *2015 6th European Symposium on Ultrasonic Characterization of Bone*, pp. 1-2, 2015.

[5] Kawasaki S., Ueda R., Hasegawa A., Fujita A., Mihata T., Matsukawa M., "Ultrasonic wave properties of human bone marrow in the femur and tibia," *The Journal of the Acoustical Society of America*, vol. 138, no. 1, 2015.

[6] Otani T., "Quantitative estimation of bone density and bone quality using acoustic parameters of cancellous bone for fast and slow waves," *Japanese Journal of Applied Physics*, vol. 44, no. 6B, 2005.

[7] Cardoso L., Teboul F., Sedel L., Oddou C., Meunier A., "In vitro acoustic waves propagation in human and bovine cancellous bone," *Journal of Bone and Mineral Research : The Official Journal of The American Society for Bone and Mineral Research*, vol. 18, no. 10, pp. 1803-1812, 2003.

[8] Nelson A. M., Hoffman J. J., Holland M. R., Miller J. G., "Single mode analysis appears to overestimate the attenuation of human calcaneal bone based on Bayesian-derived fast and slow wave mode analysis," *IEEE International Ultrasonics Symposium*, pp. 1015-1018, 2012.

[9] Nagatani Y., Mizuno K., Matsukawa M., "Two-wave behavior under various conditions of transition area from cancellous bone to cortical bone," *Ultrasonics*, vol. 54, no. 5, pp. 1245-1250, 2014.
[10] Hosokawa A., Nagatani Y., Matsukawa M., "The Fast and Slow Wave Propagation in Cancellous Bone: Experiments and Simulations," *Bone Quantitative Ultrasound: Springer*, pp. 291-318, 2011.
[11] Wear K. A., "Time-domain separation of interfering waves in cancellous bone using bandlimited deconvolution: Simulation and phantom study," *The Journal of the Acoustical Society of America*, vol. 135, no. 4, pp. 2102-2112, 2014.
[12] Wear K., Nagatani Y., Mizuno K., Matsukawa M., "Fast and slow wave detection in bovine cancellous bone in vitro using bandlimited deconvolution and Prony's method," *The Journal of the Acoustical Society of America*, vol. 136, no. 4, pp. 2015-2024, 2014.
[13] Hosokawa A., "Numerical analysis of fast and slow waves backscattered from various depths in cancellous bone," *2015 IEEE International Ultrasonics Symposium*, pp. 1-4, 2015.
[14] Hosokawa A., "Variations in reflection properties of fast and slow longitudinal waves in cancellous bone with boundary condition," *2013 IEEE International Ultrasonics Symposium (IUS)*, pp. 2076-2079, 2013.
[15] Hosokawa A., "Numerical investigation of reflection properties of fast and slow longitudinal waves in cancellous bone: Variations with boundary medium," *Japanese Journal of Applied Physics*, vol. 53, no. 7S, 2014.
[16] Molero-Armenta M., Iturrarán-Viveros U., Aparicio S., Hernández M., "Optimized OpenCL implementation of the elastodynamic finite integration technique for viscoelastic media," *Computer Physics Communications*, vol. 185, no. 10, pp. 2683-2696, 2014.
[17] Nagatani Y., Mizuno K., Saeki T., Matsukawa M., Sakaguchi T., Hosoi H., "Numerical and experimental study on the wave attenuation in bone–FDTD simulation of ultrasound propagation in cancellous bone," *Ultrasonics*, vol. 48, no. 6, pp. 607-612, 2008.
[18] Gilbert R. P., Guyenne P., Li J., "Numerical investigation of ultrasonic attenuation through 2D trabecular bone structures reconstructed from CT scans and random realizations," *Computers in Biology and Medicine*, vol. 45, pp. 143-156, 2014.
[19] Marutyan K. R., Holland M. R., Miller J. G., "Anomalous negative dispersion in bone can result from the interference of fast and slow waves," *The Journal of the Acoustical Society of America*, vol. 120, no. 5, pp. EL55-EL61, 2006.
[20] Hosokawa A., "Ultrasonic pulse waves propagating through cancellous bone phantoms with aligned pore spaces," *Japanese Journal of Applied Physics*, vol. 45, no. 5B, pp. 4697, 2006.
[21] Wear K. A., "Ultrasonic scattering from cancellous bone: A Review," *IEEE Transactions on Ultrasonics, Ferroelectrics, and Frequency Control*, vol. 55, no. 7, pp. 1432-1441, 2008.
[22] Anderson C. C., Bauer A. Q., Holland M. R., Pakula M., Laugier P., Bretthorst G. L., "Inverse problems in cancellous bone: Estimation of the ultrasonic properties of fast and slow waves using Bayesian probability theory," *The Journal of the Acoustical Society of America*, vol. 128, no. 5, pp. 2940-2948, 2010.
[23] Anderson C. C., Bauer A. Q., Marutyan K. R., Holland M. R., Pakula M., Bretthorst G. L., "Phase velocity of cancellous bone: Negative dispersion arising from fast and slow waves, interference, diffraction, and phase cancellation at piezoelectric receiving elements," *Bone quantitative ultrasound: Springer*, pp. 319-330, 2011.
[24] Lee K. I., "Relationships of linear and nonlinear ultrasound parameters with porosity and trabecular spacing in trabecular-bone-mimicking phantoms," *The Journal of the Acoustical Society of America*, vol. 140, no. 6, pp. EL528-EL33, 2016.
[25] Hoffman J. J., Nelson A. M., Holland M. R., Miller J. G., "Cancellous bone fast and slow waves obtained with Bayesian probability theory correlate with porosity from computed tomography," *The Journal of the Acoustical Society of America*, vol. 132, no. 3, pp. 1830-1837, 2012.
[26] Pakula M., "On the modeling of wave propagation in cancellous bone," *6th IEEE European Symposium on Ultrasonic Characterization of Bone (ESUCB)*, pp. 1-4, 2015.
[27] Abderrazek B., Tarek B., "Ultrasonic non-destructive characterization of trabecular bone: Experimental and theoretical prediction of the ultrasonic attenuation," *2015 3rd IEEE International Conference on Control, Engineering & Information Technology (CEIT)*, pp. 1-6, 2015.
[28] Nelson A. M., Hoffman J. J., Anderson C. C., Holland M. R., Nagatani Y., Mizuno K., "Determining attenuation properties of interfering fast and slow ultrasonic waves in cancellous bone," *The Journal of the Acoustical Society of America*, vol. 130, no. 4, pp. 2233-2240, 2011.